

High Temperature PEM Fuel Cells Based on Nafion[®]/SiO₂ Composite Membrane

XiaoJin Li, ChangChun Ke, ShuGuo Qu,
Jin Li, ZhiGang Shao and BaoLian Yi

*Laboratory of Fuel Cell System & Engineering, Dalian Institute of Chemical Physics,
Chinese Academy of Sciences,
China*

1. Introduction

1.1 High temperature PEMFC

Polymer electrolyte membrane fuel cell (PEMFC) is considered to be one of the most promising alternative energy conversion devices for motor vehicles and other stationary applications, due to its quick start, high energy efficiency, and environmentally friendly qualities (Marban and Vales-Solis 2007).

At present, most PEMFCs are operated at <80°C, due to the dependence of aboard used per-fluorinated sulfonic acid membrane (such as Nafion[®] series) on water. Even so, operating PEMFC at a high temperature (>100°C) has many benefits (Yang, Costamagna et al. 2001; Li, He et al. 2003). Firstly, it avoids the existence of two phase flow in the flow field, thus enhances the stability & reliability of PEMFCs system. Then, operating PEMFC at a high temperature reduces the power loss caused by the electrochemical polarization of cathode. In addition, high temperature operation is also beneficial to make use of the exhaust heat of PEMFC system effectively and enhance the CO endurance of anode (Yang, Costamagna et al. 2001), etc.

The key point of the HT-PEMFC is to develop a type of proton exchange membrane that can be durable to the high temperature and still maintain high proton conduction. Because the most widely used commercial Nafion membrane is not competent for operating at high temperature due to dehydration. To solve this problem, many kinds of solutions have been proposed. Generally, these solutions can be divided into three catalogs as followings: a) to incorporate hydrophilic or proton conductive inorganic nano particles into the Nafion matrix to prepare so-called inorganic-organic composite membrane (Deng, Moore et al. 1998; Adjemian, Lee et al. 2002; Adjemian, Srinivasan et al. 2002; Costamagna, Yang et al. 2002; Shao, Joghee et al. 2004; Xu, Lu et al. 2005; Yonghao Liu, Baolian Yi et al. 2005; Adjemian, Dominey et al. 2006; Shao, Xu et al. 2006; Alberti, Casciola et al. 2007; Lin, Yen et al. 2007; Casciola, Capitani et al. 2008; Jian-Hua, Peng-Fei et al. 2008; Jin, Qiao et al. 2008; Jung, Weng et al. 2008; Rodgers, Shi et al. 2008; Wang, Yi et al. 2008; Yuan, Zhou et al. 2008; Santiago, Isidoro et al. 2009; Yan, Mei et al. 2009); b) to substitute the water in Nafion with non-volatile or low-volatile polar solvent; c) to prepare new material that can conduct proton independent of water (Deng, Moore et al. 1998; Adjemian, Lee et al. 2002; Yonghao Liu, Baolian Yi et al. 2005; Lin, Yen et al. 2007; Tang, Wan et al. 2007; Yen, Lee et al. 2007; Rodgers, Shi et al. 2008).

1.2 Nafion inorganic composite membrane

During the above solutions for high-temperature operation of PEMFC, the first solution that could be also called "Nafion-inorganic composite" (Costamagna, Yang et al. 2002; Mauritz, Mountz et al. 2004; Shao, Joghee et al. 2004; Adjemian, Dominey et al. 2006; Shao, Xu et al. 2006; Jung, Weng et al. 2008; Wang, McDermid et al. 2008; Wang, Zhao et al. 2008; Yan, Mei et al. 2009) is most widely investigated at present. Many composite membranes of this type were reported in literatures, such as Nafion composite membranes with SiO₂ (Mauritz, Stefanithis et al. 1991; Shao, Joghee et al. 2004; Yonghao Liu, Baolian Yi et al. 2005; Shao, Xu et al. 2006; Tang, Wan et al. 2007; Yen, Lee et al. 2007; Jin, Qiao et al. 2008; Jung, Weng et al. 2008; Rodgers, Shi et al. 2008; Wang, McDermid et al. 2008; Yuan, Zhou et al. 2008; Jin, Qiao et al. 2009), sulfonated-SiO₂ (Wang, Zhao et al. 2008), TiO₂ (Jian-Hua, Peng-Fei et al. 2008; Santiago, Isidoro et al. 2009), and ZrP (Alberti, Casciola et al. 2007), and etc (Alberti and Casciola 2003; Jones and Rozière 2003). Among these composite membranes, Nafion/SiO₂ composite membrane was most extensively evaluated and promising, for its relative higher performance and less incidental problems. Several preparation methods have been reported, such as solution-recast route (Shao, Joghee et al. 2004), sol-gel method, self-assembling method (Tang, Wan et al. 2007), in-situ sol-gel method (Adjemian, Lee et al. 2002; Yonghao Liu, Baolian Yi et al. 2005), and so on. Among these methods, in-situ sol-gel method is a promising process route, because it could obtain composite membrane with higher uniformity, smaller SiO₂ particles and easy to carry out. K.A. Mauritz and co-workers (Mauritz, Stefanithis et al. 1991; Mauritz, Stefanithis et al. 1995) first proposed this method, then K.T. Adjemian (Adjemian, Srinivasan et al. 2001; Adjemian, Lee et al. 2002; Adjemian, Srinivasan et al. 2002) and many other investigators (Yonghao Liu, Baolian Yi et al. 2005; Yu, Pan et al. 2007) applied Nafion/SiO₂ composite membrane prepared by this or improved method to PEMFC and DMFC.

2. Nafion[®]/SiO₂ composite membrane fabrication

2.1 Membrane fabrication

Nafion/SiO₂ composite membranes were prepared via an in-situ sol-gel reaction of tetraethyl-orthosilicate (TEOS), as that of Ref (Mauritz, Stefanithis et al. 1991). In our previous work (Ke, Li et al. 2010; Ke, Li et al. 2011), a technique in controlling silicate nanoparticle diameter in preparation of Nafion/SiO₂ composite membranes was put forward. The detailed process is shown as follows. Firstly, the Nafion (NRE212) membrane (DuPont, USA) was dried in the vacuum drying oven at 80°C for 12h. Then, the membrane was dipped into the CH₃OH/H₂O solution (30°C) and kept in the CH₃OH/H₂O solution for 1 h. After that, the sample was taken out and the remnant liquid on the surface of the membrane was rubbed out with filter paper. The sample was then immersed into CH₃OH/TEOS solution (30°C) to carry out the in-situ sol-gel reaction for 3 minutes. The diameter of SiO₂ nanoparticle incorporated in Nafion was controlled by changing the in-situ sol-gel reaction reactant concentrations. After reaction, the sample was kept in the vacuum drying oven at 80°C for 48 h, and then Nafion/SiO₂ composite membrane was obtained. In this work, the content of the SiO₂ incorporated into Nafion is 8.5wt.% with a statistical diameter of 10 nm.

Before the subsequent measurements, all the composite membranes were pretreated with the process as follows. Firstly, membranes were kept in H₂O₂ (5wt%, 80°C) for 1 h, followed by rinsing them with de-ionized water (80°C) for two times. Then membranes were soaked in H₂SO₄ (0.5M, 80°C) for 1 h. Finally, membranes were rinsed with de-ionized water (80°C) repeatedly until the PH of the washing water was around 7.

For the ex-situ research of the mechanism of sulfonation, the powder of SiO₂ nano-particles was also sulfonated by concentrated H₂SO₄ (98%, 80 °C), just as the sulfonation process of Nafion/SiO₂ composite membrane. The sulfonation time was 10 h, for the powder SiO₂.

2.2 Membrane sulfonation

The above obtained Nafion/SiO₂ composite membranes were dried in vacuum drying chamber for 24 h. Then the samples were soaked in concentrated H₂SO₄ (98%, 80 °C) for certain time (4, 10, and 16 h) to sulfonate the composite membrane. The concentrated H₂SO₄ treated membranes were then soaked in de-ionized water (80 °C) for 12 h, and rinsed with de-ionized water until the washing water exhibited neutral.

Nafion/SiO₂ sulfonated for 4, 10 and 16 h are signed as Nafion/S-SiO₂-4h, Nafion/S-SiO₂-10h and Nafion/S-SiO₂-16h, respectively. For the ex-situ research of the mechanism of sulfonation, the powder of SiO₂ nano-particles was also sulfonated by concentrated H₂SO₄ (98%, 80 °C), just as the sulfonation process of Nafion/SiO₂ composite membrane. The sulfonation time was 10 h, for the powder SiO₂.

3. Spectroscopic studies of Nafion/SiO₂ composite membranes

3.1 FT-IR spectra

Spectroscopic methods are powerful tools for analysis of the chemical structure of the sample. In order to understand the mechanism of the sulfonation of the Nafion/SiO₂ composite membrane, several spectroscopic methods are used synthetically.

The FT-IR spectra of the membranes were collected from 400 cm⁻¹ to 1200 cm⁻¹, using a Bruker Vector22 (Bruker Optics, Germany) FT-IR spectrometer at a resolution of 4 cm⁻¹ in absorption mode. FT-IR of the powder SiO₂ and sulfonated SiO₂ (S-SiO₂) nano-particles were also performed, in order to avoid the background signal of the Nafion matrix. The IR spectra of the untreated SiO₂ and the sulfonated S-SiO₂ were recorded with potassium bromide tableting in transmission mode.

Figure 1 (a) exhibits the FT-IR spectra of the Nafion, Nafion/SiO₂, Nafion/S-SiO₂-4h, Nafion/S-SiO₂-10h, and Nafion/S-SiO₂-16h. In fact, as we can see, it is a little difficult to distinguish the structure change of the Nafion/SiO₂ composite membrane after sulfonation from Figure 1 (a). This maybe caused by -SO₃H groups in the side chains of Nafion, which is much adverse for the identification of the -SO₃H that maybe attached to the surface of SiO₂ nano particles. Therefore, in this experiment, an ex-situ characterization method was adopted. Powder SiO₂ nano-particles were prepared outside the Nafion membrane via a sol-gel reaction of TEOS. Then the obtained SiO₂ was sulfonated (signed as S-SiO₂) by concentrated H₂SO₄ for 10 h at 80 °C as mentioned in section 2.2.

Figure 1 (b) illustrates the spectra of the obtained SiO₂ and sulfonated S-SiO₂. It is shown that the peak at 3400 cm⁻¹, which is the characteristic signal of -OH, is widened after sulfonation. It is generally acknowledged that the widening of the hydroxyl peak is caused by the hydrogen bond. It suggests that there are strong hydrogen bonds in the sulfonated S-SiO₂. This should be caused by the interaction between surface -OH groups of SiO₂ nano-particles and H₂SO₄ molecules. However, characteristic peaks of the -SO₃H group are located in 1000-1100 cm⁻¹, which coincides with the strong absorption band of symmetric and anti-symmetric vibration of the Si-O-Si. For this reason, the structure signal of -SO₃H is not clear by FT-IR.

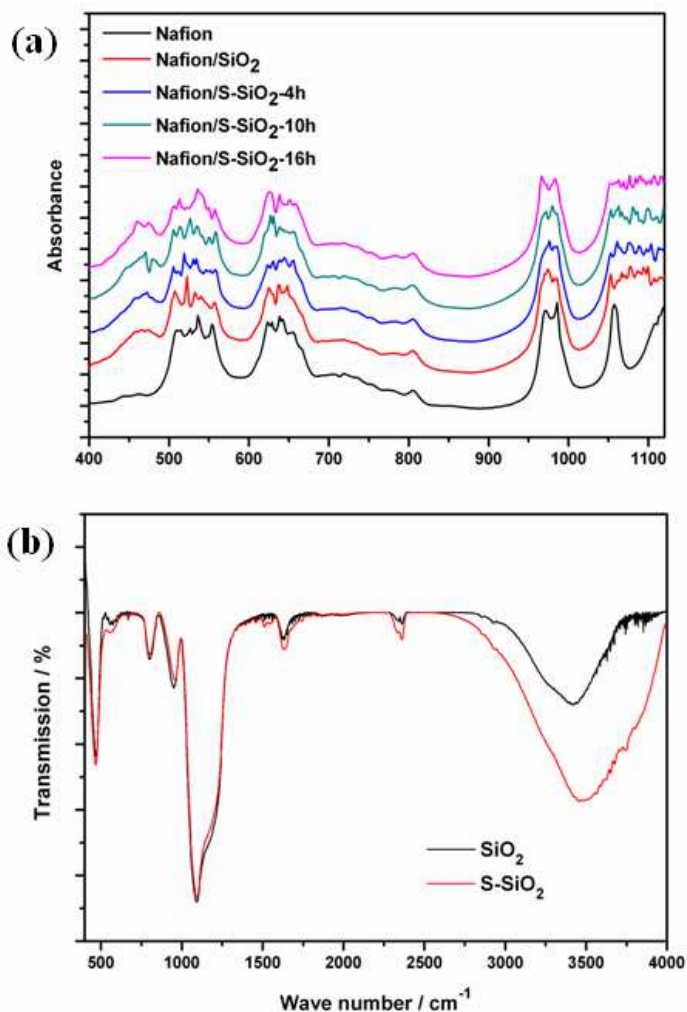


Fig. 1. (a) FT-IR spectra of Nafion, Nafion/SiO₂ and sulfonated Nafion/S-SiO₂ composite membranes; (b) FT-IR spectra of sol-gel derived SiO₂ and the sulfonated S-SiO₂. (Ke, Li, et al., 2011)

3.2 UV Raman spectra

UV resonance Raman spectra were recorded at room temperature using a home-made UV resonance Raman spectrograph of State Key Laboratory of Catalysis (Dalian institute of Chemical Physics) at a resolution of 2 cm⁻¹. The laser line at 325 nm of a He-Cd laser was used as an exciting source with an output of 25 mW.

From FT-IR, it suggests the existence of strong hydrogen bond in the S-SiO₂. However, whether the -SO₃H groups are chemically attached to the surface of the SiO₂ nano-particles, or how the -SO₃H groups interact with SiO₂ nano-particles remains unclear. UV resonance

Raman spectroscopy (UVRRS) is a powerful tool for surface species detection & identification. Therefore, in this experiment the UVRRS spectra of SiO₂ and S-SiO₂ were recorded, using a home-made UV Raman Resonance Spectrograph. The UVRRS spectra of SiO₂ and S-SiO₂ are shown as Figure 2. It can be seen that the scattering pattern of SiO₂ is much different from that of the sulfonated S-SiO₂. For the scattering pattern of the sulfonated S-SiO₂, the peaks at 873 cm⁻¹ and ~620 cm⁻¹ disappear, and a new peak at 710 cm⁻¹ emerges. Besides, the band around 400 cm⁻¹ is broadened after sulfonation.

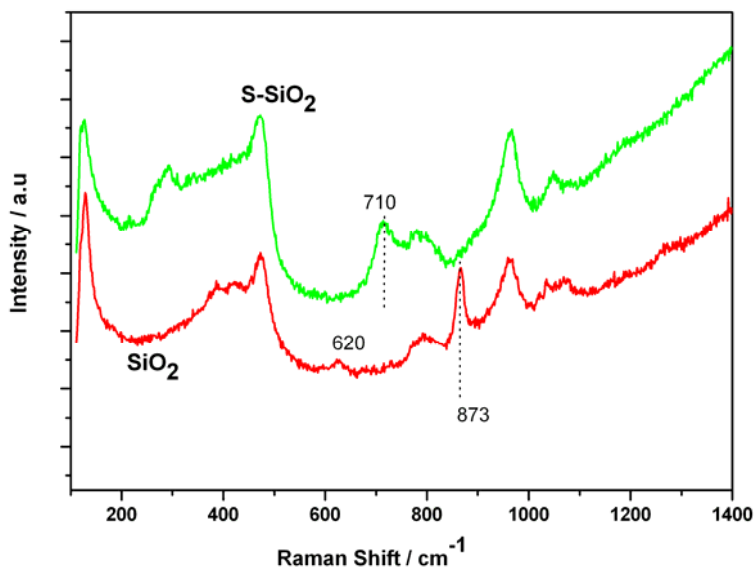


Fig. 2. UV Raman spectra of sol-gel derived SiO₂ and the sulfonated S- SiO₂. (Ke, Li, et al., 2011)

It is well known, the scattering peaks at ~620 cm⁻¹ and 873 cm⁻¹ could be attributed to the so called D2 defect structure (strained three-membered rings) and strained 2-fold rings (edge-sharing tetrahedra) respectively (Brinker, Kirkpatrick et al. 1988), which form primarily on the silica surface by condensation reactions involving isolated adjacent silanol groups (Brinker, Tallant et al. 1986). After sulfonation, the ~620 cm⁻¹ and 873 cm⁻¹ peaks disappear, suggesting that a reverse reaction of surface condensation occurs during sulfonation. And the new peak at 710 cm⁻¹ should be due to the new surface specie (Si-O-SO₃H) forming.

From the UVRRS results, it is clearly seen that sulfonation affects the surface structure of the SiO₂ nano-particles to a large degree. The chemical bond assembled between sulfonic group and SiO₂ nano-particles is responsible for covering the proton conductivity loss of the Nafion/SiO₂ composite membrane.

4. Physic-chemical properties of Nafion/SiO₂ composite membranes

4.1 Water uptake

For the water-uptake evaluation, to remove the residual water, the membrane was firstly dried in vacuum drying oven for 12 h at 60°C. Then, the membrane was quickly taken out

from the oven and weighed precisely. The weight of the dry membrane was signed as W_{dry} . After that, the membrane was soaked in de-ionized water at certain temperature (40°C, 60°C, or 80°C) for 24h. The weight of the wet membrane was signed as W_{wet} . The water-uptake (W_u) can be calculated by the following equation:

$$W_u = \frac{W_{wet} - W_{dry}}{W_{dry}} \times 100\% \quad (1)$$

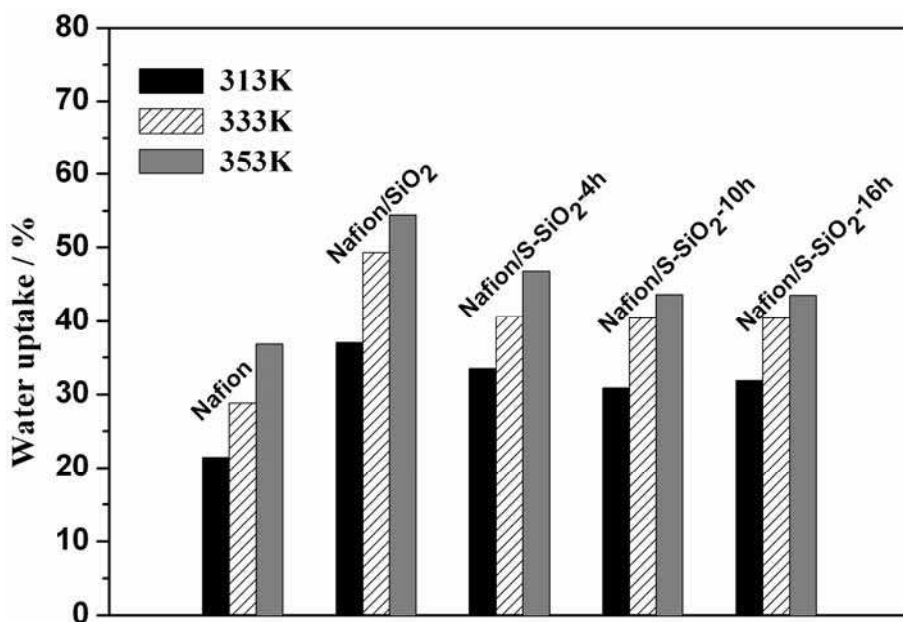


Fig. 3. Water uptakes of Nafion, Nafion/SiO₂ and Nafion/S-SiO₂ composite membranes sulfonated for 4h, 10h, and 16h. (Ke, Li, et al., 2011)

The water uptakes of Nafion, Nafion/SiO₂, Nafion/S-SiO₂-4h, Nafion/S-SiO₂-10h, and Nafion/S-SiO₂-16h at 40, 60, and 80 °C are shown in Figure 3. It shows that the Nafion/SiO₂ has a higher water uptake than the unmodified Nafion at the considering temperature region. At the temperature of 80 °C, the water uptake of the Nafion is 35%, while Nafion/SiO₂ has water up take of 56%, much higher than that of the unmodified Nafion. That should attribute to the hydrophilicity of the SiO₂ nano particles, of which the surface -OH groups have excellent capability of water maintenance. However, after treatment with concentrated sulfuric acid, the water uptake of the composite membrane decreases. And, it descends synchronously as the sulfonation time ascends.

4.2 Proton conductivity

Electrochemical Impedance Spectroscopy (EIS) was carried out to measure the proton conductivities of the membranes, using a Solartron impedance/Gain-phase Analyzer (model SI 1260) combined with a Solartron Electrochemical Interface (model SI 1287). Z-plot

and Z-view software were used to control the measurement process. The amplitude of the AC signal was 20 mV, and the frequency was set from 100 Hz to 1 MHz. All samples were soaked in de-ionized water at 40 °C for 24 h and then sealed between two carbon-paper electrodes with an area of 0.332 cm² for measurement. The conductivity could be calculated using the following equation:

$$\sigma = \frac{L}{R \times A} \quad (2)$$

Where, σ is the proton conductivity of the membrane, R is the resistance of the membrane, and the sign L as well as A stands for the thickness of the membrane and the area of the electrode, respectively.

The EIS plots of the membranes are shown as Figure 4. It could be seen that the membrane resistance of Nafion/SiO₂ is higher than that of the unmodified Nafion. It suggests that SiO₂ nano-particles incorporated into the Nafion matrix block the conduction of protons. Therefore, in this chapter we sulfonated the Nafion/SiO₂ composite membrane on the purpose to cover the conductivity loss caused by the SiO₂. In Figure 4, it could be seen that the membrane resistances of the Nafion/S-SiO₂ (4h, 10h, and 16h) composite membranes are lower than that of the un-sulfonated Nafion/SiO₂ composite membrane. It proves that the sulfonation is an effective method to cover the shortcoming of Nafion/SiO₂ composite membrane on proton conductivity.

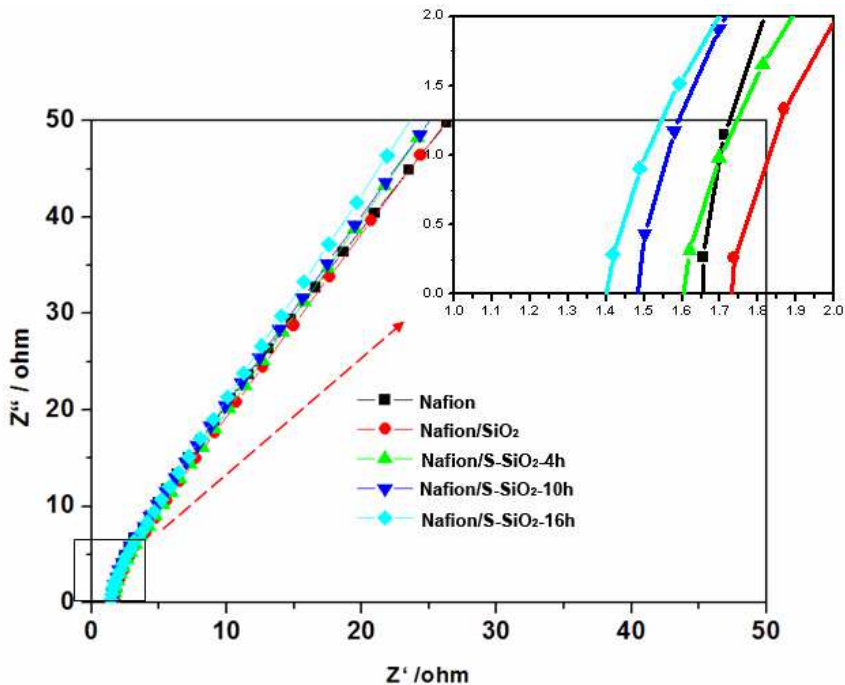


Fig. 4. Proton conductivities of Nafion, Nafion/SiO₂ and Nafion/S-SiO₂ composite membranes sulfonated for 4h, 10h, and 16h. (Ke, Li, et al., 2011)

4.3 Diffusion coefficient of water

Water transport in the Nafion membrane influences the proton transport in the membrane (Sumner, Creager et al. 1998; Inzelt, Pineri et al. 2000), so it is important to understand the transport process in the fuel cell. Water balance in the membrane depends on the interaction among the three kind of water transmission mechanisms---electroosmosis, back diffusion and hydraulic permeation. Membrane water diffusion coefficient as the PEMFC water transmission process's key parameter has attracted many attentions (Nguyen and White 1993; Zawodzinski, Jr. et al. 1993; Motupally and Becker 2000). However, most of the studies were based on the Nafion membrane. Researches on the water diffusion coefficient in the modified Nafion membrane are few. Nicotera (Nicotera, Zhang et al. 2007; Nicotera, Khalfan et al. 2008) et al used pulse gradient field spin echo nuclear magnetic resonance technology (PFGSE-NMR) obtain the water diffusion coefficient of the recast Nafion/SiO₂ composite membrane, but they did not connect the composite membrane waters' diffusion coefficient with the SiO₂ content and the temperature. In this work, the diffusion coefficient of water across the Nafion212/SiO₂ composite membranes with different SiO₂ content were measured through steady state permeation, and an empirical correlation of the water apparent diffusion coefficient of Nafion212/SiO₂ composite membrane as a function of SiO₂ content and temperature was presented.

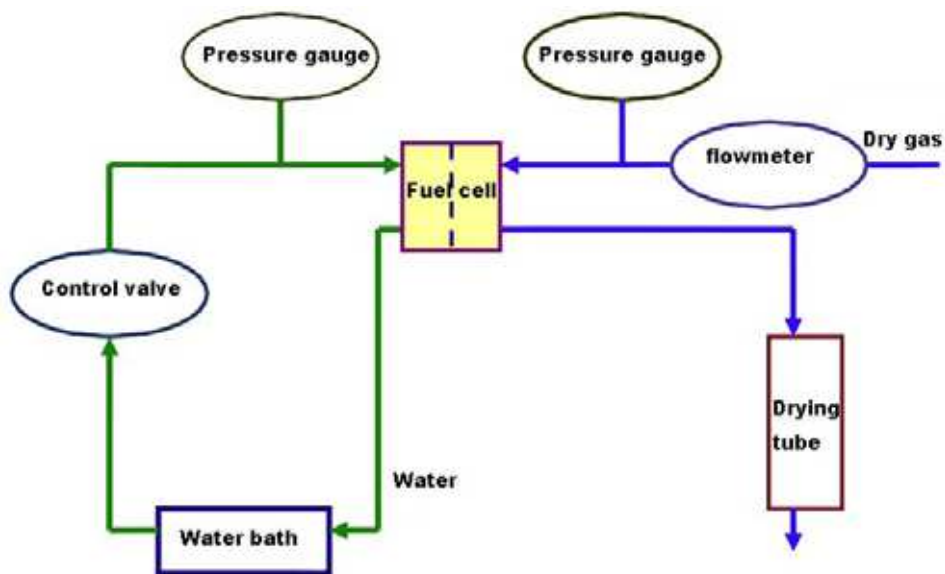


Fig. 5. Scheme of the experimental setup

A pseudo fuel cell, consisting of the measured membrane sandwiched between two GDLs, was used to measure the water flux through the membrane. Figure 5 is the scheme of the experimental setup. In the process, preheated water was circulated through one side of the fuel cell and dry air passed through the other side. As the gas traversed the length of the cell, its humidity increased due to the diffusion of water across the membrane. To

measure the amount of water diffusion across the composite membrane, the air exiting the cell was passed through a tube filled with silica gel. Gravimetric analysis was conducted by precision analytical balance. The temperatures of intake air, the preheated water and the fuel cell were kept consistent. Water flux through the composite membrane under different operating conditions was measured by adjusting the air flow rate and temperature. In the experiment, water diffusion coefficients of Nafion/SiO₂ composite membranes with weight content of silica from 7.8% to 16.6% were measured and the area of the pseudo fuel cell is 5 cm².

Figure 6 displayed the water flux through the Nafion212/SiO₂ composite membrane with different content of SiO₂ as a function of the inlet gas flow rate of air at different operating temperatures. From this figure, the water flux through the composite membrane increases with the increasing of the temperature. At the same temperature, the water flux through the composite membrane increases with the increasing of the SiO₂ content, which may be caused by the water apparent diffusion coefficient.

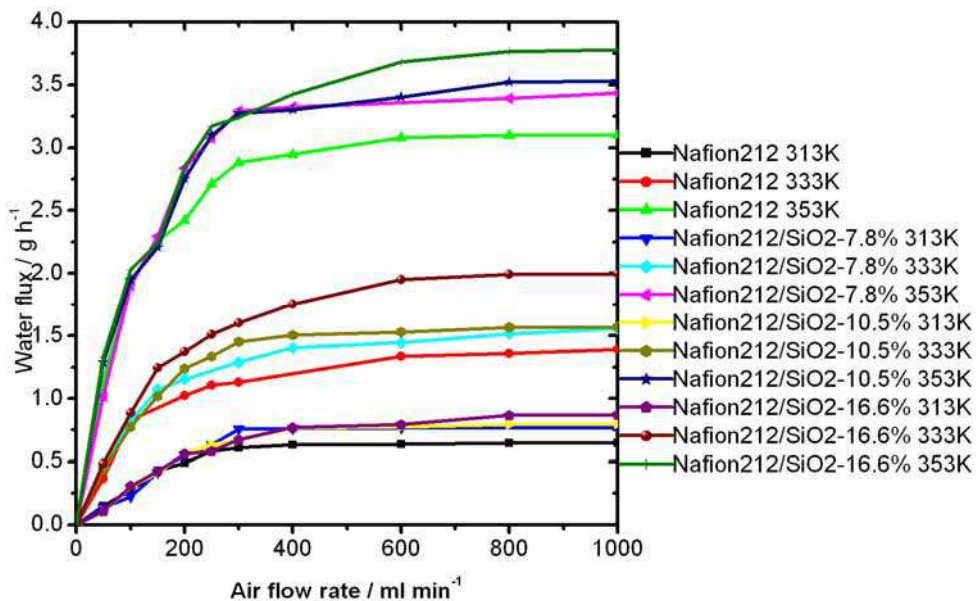


Fig. 6. Water flux of Nafion212/SiO₂ composite membrane with different content of SiO₂ as a function of the inlet gas flow rate of air at different operating temperatures. (Qu, Li, et al., 2011)

Assumed that the water transfer across the membrane was the control step, the water concentration gradient across the membrane was the driving force for the water diffusion. According to the Fick's first law, the water diffusion flux was

$$J = D_w \frac{c_{w,a} - c_{w,g}}{\delta_m} \quad (3)$$

where J is water flux, D_w water apparent diffusion coefficient, δ_m membrane thickness, $c_{w,a}$ pure water concentration, 55.6 mol/l, $c_{w,g}$ water concentration in the air.

The water flux across the composite membrane was measured at the air flow rate of 800ml/min under temperature from 303 to 353K. The water apparent diffusion coefficient calculated from Eq. 3 was showed in Figure 7. It was clearly seen that the water apparent diffusion coefficient of Nafion212 membrane was lower than that of Nafion/SiO₂ composite membrane, and the diffusion coefficient of composite membrane increased with the increase of SiO₂ content.

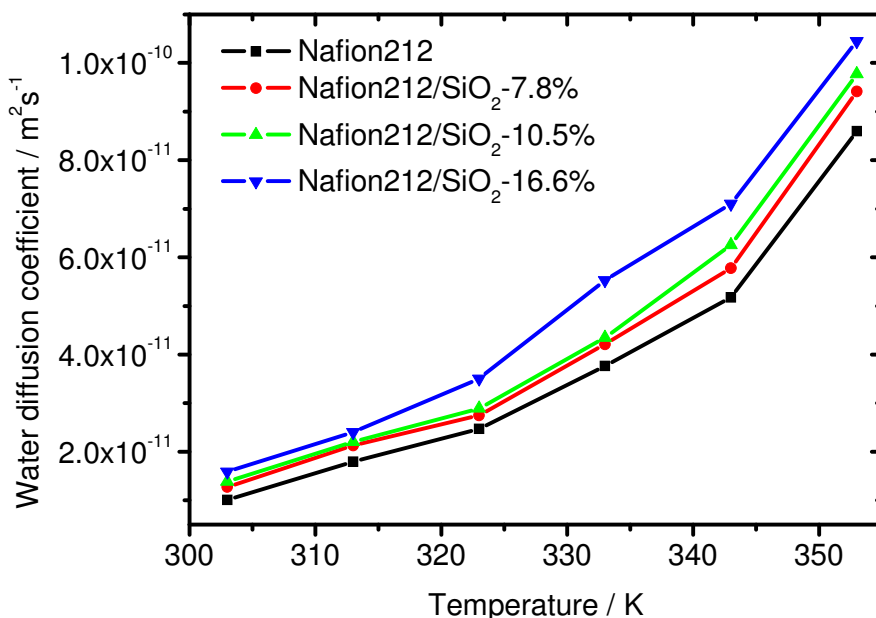


Fig. 7. The water apparent diffusion coefficient of Nafion212/SiO₂ composite membrane with different content of SiO₂ as a function of temperature. (Qu, Li, et al. , 2011)

Assumed that the water apparent diffusion coefficient of the Nafion212/SiO₂ composite membrane and temperature were consistent with Arrhenius equation, that was

$$\ln D_w = \ln D_0 - \frac{E_a}{RT} \quad (4)$$

Equation (4) was carried on the linear regression to Nafion212/SiO₂ composite membrane's $\ln D_w$ and $1000/T$, as shown in Figure 8. The results showed that the $\ln D_w$ was linear correlation with $1000/T$ in the temperature range from 303 to 353K. This demonstrated that the assumption was right. The apparent diffusion activation energy (E_a) and pre-exponential factor of the composite membrane was obtained through linear fit in Figure 8, listed in Table 1. The apparent diffusion activation energy of the Nafion212 membrane was higher than that of the Nafion212/SiO₂ composite membrane, indicated that water diffusion was easier in the Nafion212/SiO₂ composite membrane.

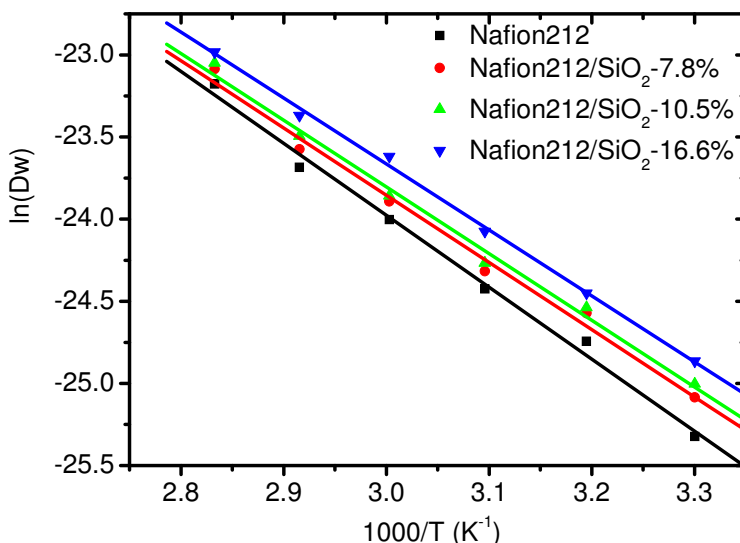


Fig. 8. Arrhenius plot of water apparent diffusion coefficient of Nafion212/SiO₂ composite membrane with different content of SiO₂ (Qu, Li, et al. , 2011)

	$E_a / \text{KJ mol}^{-1}$	$D_0 / \text{m}^2 \text{s}^{-1}$
Nafion212	36.43	1.977×10^{-5}
Nafion212/SiO ₂ -7.8%	34.03	9.398×10^{-6}
Nafion212/SiO ₂ -10.5%	33.77	8.999×10^{-6}
Nafion212/SiO ₂ -16.6%	33.36	8.939×10^{-6}

Table 1. Apparent activation energy and pre-exponential factor of composite membrane

Associate the apparent activation energy and the pre-exponential factor of composite membrane with the SiO₂ content, getting the following relationship

$$E_a = 33.16882 + 3.25989 \exp\left(-\frac{W_{\text{SiO}_2}}{0.05989}\right) \tag{5}$$

$$D_0 = 8.89161 \times 10^{-6} + 1.08831 \times 10^{-5} \exp\left(-\frac{W_{\text{SiO}_2}}{0.02504}\right) \tag{6}$$

Then the empirical correlation of apparent diffusion coefficient of the Nafion212/SiO₂ composite membrane was

$$D_w = \left(8.89161 \times 10^{-6} + 1.08831 \times 10^{-5} \exp\left(-\frac{W_{\text{SiO}_2}}{0.02504}\right) \right) \exp\left(-1000 \left(33.16882 + 3.25989 \exp\left(-\frac{W_{\text{SiO}_2}}{0.05989}\right) \right) / RT\right) \left(\text{m}^2 / \text{s} \right) \tag{7}$$

The comparison of water apparent diffusion coefficient of the Nafion212/SiO₂ composite membrane calculated using this empirical correlation and the experimental data was shown in Figure 9, with a difference in less than 10%. Therefore this empirical correlation can be used to represent the relationship between the water apparent diffusion coefficient of the Nafion212/SiO₂ composite membrane and SiO₂ content and temperature.

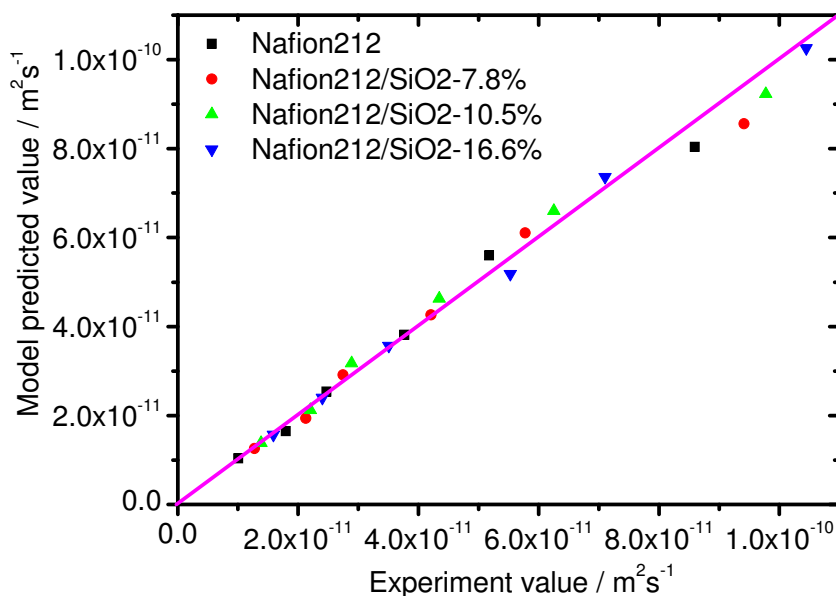


Fig. 9. Comparison of the empirical correlation predicted and experimental water apparent diffusion coefficient of composite membrane. (Qu, Li, et al. , 2011)

5. High temperature PEM fuel cell technologies

5.1 Fuel cell performance

All membrane electrode assemblies (MEAs) were prepared via a hot-pressing process. The Gas Diffused Electrode (GDE) was prepared first. In preparation of GDE, carbon paper from Toray, 20wt.% Pt/C from E-TEK, PTFE suspension and Nafion solution (DuPont, USA) were used. Carbon powder and PTFE suspension (DuPont, USA) were well mixed with ethanol under ultrasonic for 30 min, and spray-coated on side of the previous PTFE-treated carbon paper (Toray, Japan). The carbon paper was desiccated at 245 °C for 30min to eliminate the surfactant of PTFE suspension, and then 350 °C for 1 h. Catalyst inks were prepared by mixing 20wt.% Pt/C (E-TEK), 5 wt.% Nafion solution, and isopropanol. The mixture was sonicated for 30min and spray-deposited onto the carbon powder layer of the above treated carbon paper. Then the carbon paper was desiccated at 245 °C for 30min to eliminate the residual solvent, and then 350 °C for 1 h. Finally, Nafion solution (~2% with ethanol) was spray-deposited on to the catalyst layer. After dried at 100 °C for 2 h, the electrode is obtained. The contents of Nafion and PTFE in the catalyst layer are both 23.6 wt. %.

Both the loadings of Pt/C catalyst on the anode and cathode were 0.4 mgPt.cm⁻². Then, two pieces of gas diffused electrode with effective area of 5 cm² were hot-pressed onto one piece

of membrane to fabricate an MEA. The MEA was sandwiched into a single cell with stainless steel end plates and graphite groove flow fields as current collectors. The performance of the fuel cell was evaluated by polarization curve measurement at the temperatures of 60°C and 110°C, respectively. The H₂ and O₂ were fed into the fuel cell in co-flow mode. When the cell was operated at the temperature of 60°C with fully humidified H₂/O₂ gases, the flow rates of inlet gases were adjusted with current density to maintain the utilization of H₂ at 70% and O₂ at 40% for various current densities. When the cell was operated at the temperature of 110°C with H₂/O₂ gases and the relative humidity (RH) of 59%, the inlet gases were controlled at fixed flow rates of 35 and 100ml.min⁻¹ respectively. All MEAs were evaluated under an absolute pressure of 0.3 MPa.

Figure 10 gives the I-V curves of these membranes: Nafion NRE212, Nafion/SiO₂, Nafion/S-SiO₂-4h, Nafion/S-SiO₂-10h, and Nafion/S-SiO₂-16h. It can be seen from the Figure 10 shows that the PEMFC single cell performance of each of the three sulfonated Nafion/S-SiO₂ membranes is enhanced compared to that of the un-treated Nafion/SiO₂ during almost the whole considering current density range, at 110 °C and 59% RH. Particularly, in the high current density region above 800 mA cm⁻², Nafion/S-SiO₂ outperforms the un-treated Nafion/SiO₂ significantly. At the current density of 1000 mA cm⁻², the output voltage is measured as 0.598, 0.690, and 0.667V when the Nafion/SiO₂ membrane is sulfonated for 4, 10, and 16 h, respectively. While for the untreated Nafion/SiO₂, the output voltage is 0.587 V at the same current density. It demonstrates that sulfonation is obviously beneficial to the elevated temperature & low humidity performance of the membranes.

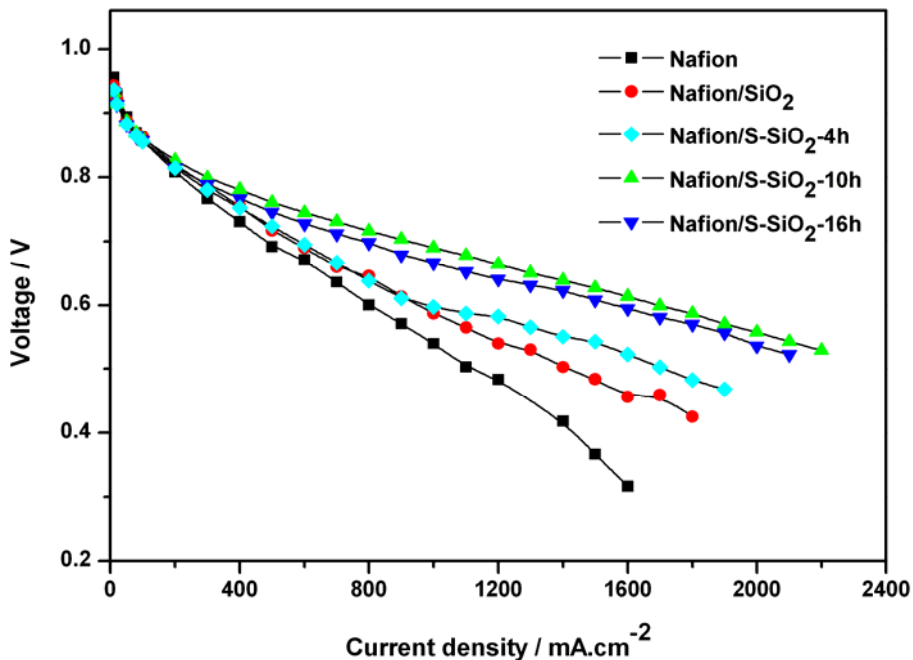


Fig. 10. I-V curves of Nafion, Nafion/SiO₂ and sulfonated Nafion/S-SiO₂ composite membranes at 110 °C, 59%RH.

5.2 High temperature PEMFC system

The fuel cell system consists of gas supply subsystem, water and heat management subsystem, fuel cell stack, automatic control subsystem. A ten-cell stack based on sulfonation Nafion/S-SiO₂-10h composite membrane was used in the fuel cell system, with single cell surface active area of 276 cm². 90% (vol) glycol water solution was used as coolant in the heat management system, which has a boiling point of 140.6 °C.

Figure 11 gives assembled high temperature PEMFCs system.

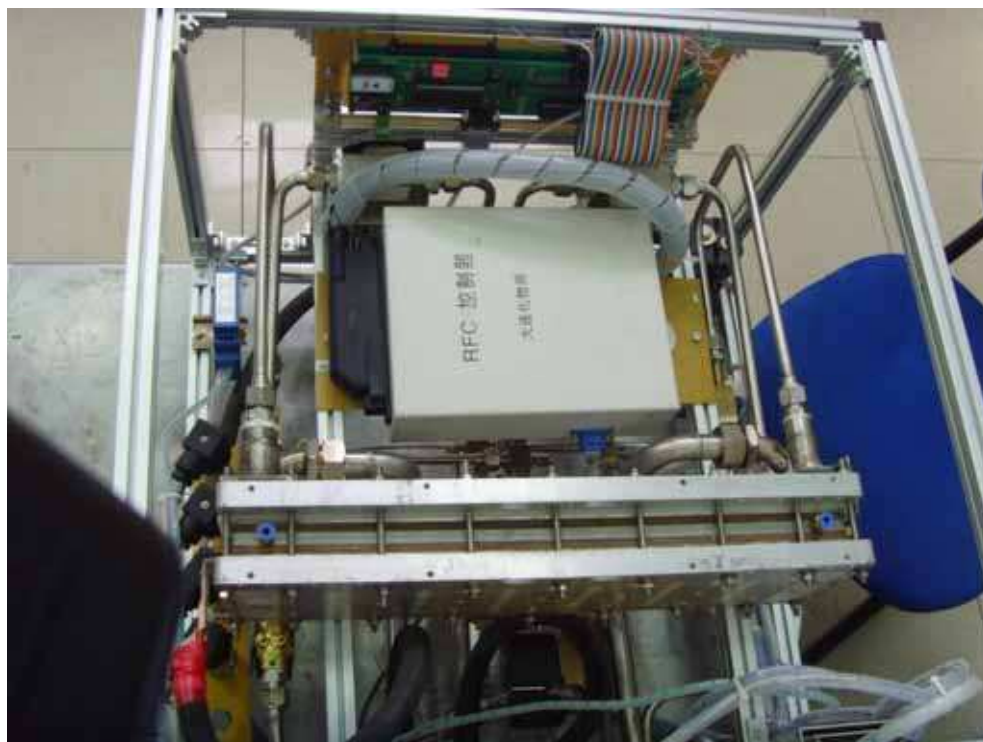


Fig. 11. Assembled high temperature PEMFCs system

Operate condition	content
Oxygen inlet	No humidification, 0.3 MPa (gauge pressure)
Hydrogen inlet	No humidification, 0.3 MPa (gauge pressure)
Cooling medium	90 % glycol water solution
Operate temperature	110 °C
Usage rate of hydrogen	≥98 %
Usage rate of oxygen	≥98 %

Table 2. The operate parameter of the high temperature PEMFCs system

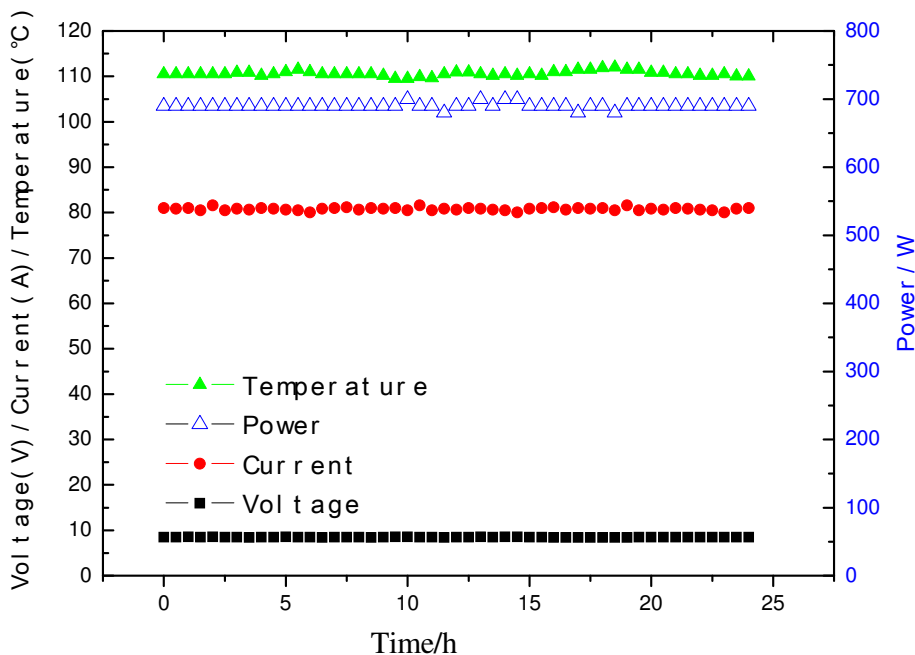


Fig. 12. Stabilization testing of the high temperature PEMFCs (H₂/O₂)

Table 2 gives the operate parameter of the high temperature PEMFCs system operating with H₂/O₂. Figure 12 gives stabilization testing of the high temperature PEMFCs operating. From Figure 12, the performance of fuel cell stack based on Nafion/S-SiO₂-10h composite membrane showed good stability under high operating temperature. The fuel cell system is also running with hydrogen and air. Table 3 gives the operate parameters of the system with H₂/Air.

Operate condition	content
Air inlet	0.25 MPa, saturation humidification at 90 °C
Hydrogen inlet	0.27 MPa, Saturation humidification at 35 °C
Cooling medium	90 % glycol water solution
Operate temperature	110 °C
Usage rate of hydrogen	≥98 %
Usage rate of air	≥50 %

Table 3. The operate parameter of the high temperature PEMFCs system

Figure 13 gives stabilization testing of the high temperature PEMFCs operating at 110 °C. From Figure 13, the fluctuation of temperature is 110 °C±3 °C, the fluctuation of voltage is 5.75±0.25 V, 600±20 W for the power, and 108±0.5 A for the current. The fluctuation of the fuel cell stack's parameter is bigger than the system operating with hydrogen and oxygen, mainly due to the unsteady humidification. However, the performance of the fuel cell stack shows no significant degradation

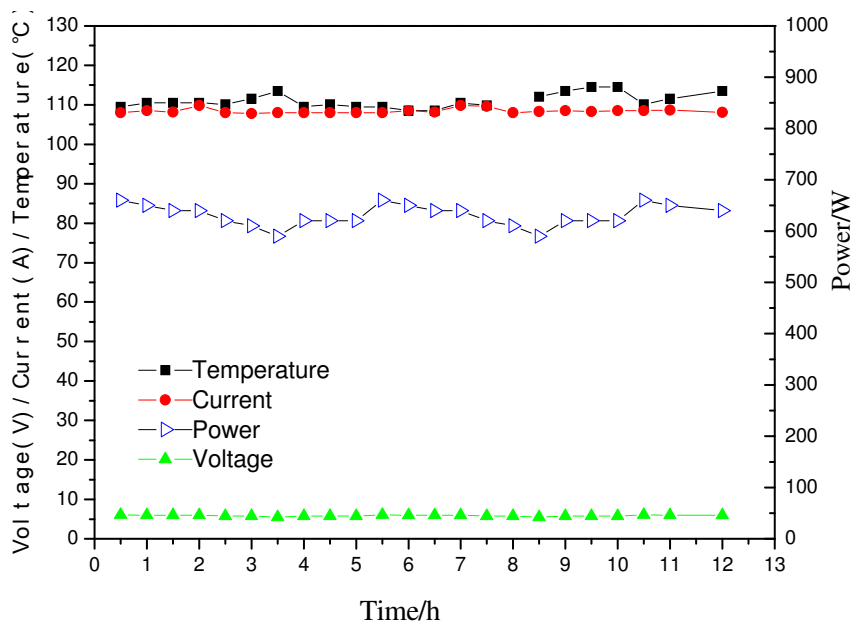


Fig. 13. Stabilization testing of the high temperature PEMFCs (H_2 /air)

From the high temperature PEMFCs system testing in this work, no significant degradation of fuel cell performance was observed. However, further life-testing is required for investigating the mechanism of composite membrane degradation under high operating temperature.

6. Conclusion

The sulfonated Nafion/ SiO_2 composite membranes were prepared by sulfonation of Nafion/ SiO_2 composite membranes with concentrated sulfuric acid. Compared to untreated Nafion/ SiO_2 , the sulfonated Nafion/ SiO_2 composite membranes have lower water uptake and higher proton conductivities. The lower water uptake of sulfonation Nafion/ SiO_2 composite membrane is due to the partly elimination of the surface -OH groups of the SiO_2 nano-particles. And, the high proton conductivity of Nafion/S- SiO_2 composite membranes can be well explained by the formation of the chemical bonds between $-SO_3H$ and the surface of SiO_2 nano-particles

The diffusion fluxes of water across the Nafion212/ SiO_2 composite membranes with different SiO_2 content were measured through steady state permeation. An empirical correlation of the water apparent diffusion coefficient of Nafion212/ SiO_2 composite membrane as a function of SiO_2 content and temperature was obtained.

Single cells based on Nafion/ SiO_2 composite membranes have been tested at temperature of up to $110^\circ C$ and compared with the experimental results based on sulfonation Nafion/ SiO_2 composite membranes. Single cell tests show that the performance of Nafion/S- SiO_2 composite membranes substantially exceeds Nafion/ SiO_2 at $110^\circ C$ and 59%RH, and in the initial testing stage no performance reduction is observed.

Related fuel cell system technologies have been further developed, especially on water and heat management and an experimental high temperature PEMFC system has been integrated based on a 10-cell stack with a single cell active area of 276 cm². From the test results, the system show good reliability and maneuverability, and fuel cells show good stability and uniformity.

7. Acknowledgement

The authors thank for the joint support by the National High Technology Research and Development Program of China (863 Program No. 2007AA05Z131) and the National Natural Science Foundation of China (No. 20206030).

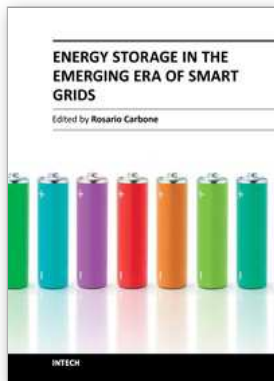
8. References

- Adjemian, K. T., Dominey, R., et al. (2006). Function and characterization of metal oxide-nafion composite membranes for elevated-temperature H₂/O₂ PEM fuel cells. *Chemistry of Materials*, Vol.18,No.9,pp. 2238-2248
- Adjemian, K. T., Lee, S. J., et al. (2002). Silicon oxide Nafion composite membranes for proton-exchange membrane fuel cell operation at 80-140 degrees C. *Journal of the Electrochemical Society*, Vol.149,No.3,pp. A256-A261
- Adjemian, K. T., Srinivasan, S., et al. (2002). Investigation of PEMFC operation above 100 degrees C employing perfluorosulfonic acid silicon oxide composite membranes. *Journal of Power Sources*, Vol.109,No.2,pp. 356-364
- Adjemian, K. T., Srinivasan, S., et al. (2001). Investigation of proton-exchange membrane fuel cells operating above 100 degrees C. *Abstracts of Papers of the American Chemical Society*, Vol.221,No.U382-U382
- Alberti, G. and Casciola, M. (2003). Composite membranes for medium-temperature PEM fuel cells. *Annual Review of Materials Research*, Vol.33,No.129-154
- Alberti, G., Casciola, M., et al. (2007). Novel Nafion-zirconium phosphate nanocomposite membranes with enhanced stability of proton conductivity at medium temperature and high relative humidity. *Electrochimica Acta*, Vol.52,No.28,pp. 8125-8132
- Brinker, C. J., Kirkpatrick, R. J., et al. (1988). Nmr Confirmation of Strained Defects in Amorphous Silica. *Journal of Non-Crystalline Solids*, Vol.99,No.2-3,pp. 418-428
- Brinker, C. J., Tallant, D. R., et al. (1986). Sol-Gel Transition in Simple Silicates .3. Structural Studies during Densification. *Journal of Non-Crystalline Solids*, Vol.82,No.1-3,pp. 117-126
- Casciola, M., Capitani, D., et al. (2008). Nafion-zirconium phosphate nanocomposite membranes with high filler loadings: Conductivity and mechanical properties. *Fuel Cells*, Vol.8,No.3-4,pp. 217-224
- Costamagna, P., Yang, C., et al. (2002). Nafion (R) 115/zirconium phosphate composite membranes for operation of PEMFCs above 100 degrees C. *Electrochimica Acta*, Vol.47,No.7,pp. 1023-1033
- Deng, Q., Moore, R. B., et al. (1998). Nafion (R) (SiO₂, ORMOSIL, and dimethylsiloxane) hybrids via in situ sol-gel reactions: Characterization of fundamental properties. *Journal of Applied Polymer Science*, Vol.68,No.5,pp. 747-763
- Inzelt, G., Pineri, M., et al. (2000). Electron and proton conducting polymers: recent developments and prospects. *Electrochimica Acta*, Vol.45,No.15-16,pp. 2403-2421

- Jian-Hua, T., Peng-Fei, G., et al. (2008). Preparation and performance evaluation of a Nafion-TiO₂ composite membrane for PEMFCs. *International Journal of Hydrogen Energy*, Vol.33, No.20, pp. 5686-5690
- Jin, Y. G., Qiao, S. Z., et al. (2009). Porous Silica Nanospheres Functionalized with Phosphonic Acid as Intermediate-Temperature Proton Conductors. *Journal of Physical Chemistry C*, Vol.113, No.8, pp. 3157-3163
- Jin, Y. G., Qiao, S. Z., et al. (2008). Novel Nafion composite membranes with mesoporous silica nanospheres as inorganic fillers. *Journal of Power Sources*, Vol.185, No.2, pp. 664-669
- Jones, D. J. and Rozière, J. (2003). In Handbook of Fuel Cells - Fundamental, Technology and Applications. Vielstick, W. Gasteiger, H.A. Lamm, A. Eds. John Wiley & Sons: New York, Vol.3, No.447-455
- Jung, G. B., Weng, F. B., et al. (2008). Nafion/PtFE/silicate membranes for high-temperature proton exchange membrane fuel cells. *International Journal of Hydrogen Energy*, Vol.33, No.9, pp. 2413-2417
- Ke, C.C., Li, X.J., et al. (2010). Preparation and properties of Nafion/SiO₂ composite membrane derived via in situ sol-gel reaction: size controlling and size effects of SiO₂ nano-particles. *Polymers for Advanced Technologies*. doi:10.1002/pat.1828
- Ke, C.C., Li, X.J., et al. (2011). Investigation on sulfuric acid sulfonation of in-situ sol-gel derived Nafion/SiO₂ composite membrane. *International Journal of Hydrogen Energy*, Vol.36, No.5, pp. 3606-3613
- Li, Q. F., He, R. H., et al. (2003). Approaches and recent development of polymer electrolyte membranes for fuel cells operating above 100 degrees C. *Chemistry of Materials*, Vol.15, No.26, pp. 4896-4915
- Lin, Y. F., Yen, C. Y., et al. (2007). High proton-conducting Nafion (R)/-SO₃H functionalized mesoporous silica composite membranes. *Journal of Power Sources*, Vol.171, No.2, pp. 388-395
- Marban, G. and Vales-Solis, T. (2007). Towards the hydrogen economy? *International Journal of Hydrogen Energy*, Vol.32, No.12, pp. 1625-1637
- Mauritz, K. A., Mountz, D. A., et al. (2004). Self-assembled organic/inorganic hybrids as membrane materials. *Electrochimica Acta*, Vol.50, No.2-3, pp. 565-569
- Mauritz, K. A., Stefanithis, I. D., et al. (1995). Microstructural Evolution of a Silicon-Oxide Phase in a Perfluorosulfonic Acid Ionomer by an in-Situ Sol-Gel Reaction. *Journal of Applied Polymer Science*, Vol.55, No.1, pp. 181-190
- Mauritz, K. A., Stefanithis, I. D., et al. (1991). Microstructural Evolution of a Silicon-Oxide Phase in Nafion Membranes by an Insitu Sol-Gel Reaction. *Abstracts of Papers of the American Chemical Society*, Vol.202, No.285-POLY
- Motupally, S. and Becker, A. J. (2000). Diffusion of water in Nafion 115 membranes. *Journal of the Electrochemical Society*, Vol.147, No.9, pp. 3171-3177
- Nguyen, T. V. and White, R. E. (1993). A Water and Heat Management Model for Proton-Exchange-Membrane Fuel Cells. *Journal of the Electrochemical Society*, Vol.140, No.2178-2186
- Nicotera, I., Khalfan, A., et al. (2008). NMR investigation of water and methanol mobility in nanocomposite fuel cell membranes. *Ionics*, Vol.14, No.3, pp. 243-253

- Nicotera, I., Zhang, T., et al. (2007). NMR characterization of composite polymer membranes for low-humidity PEM fuel cells. *Journal of the Electrochemical Society*, Vol.154,No.B466-B473
- Qu, S.G., Li, X. J., et al. (2011). Investigation on water diffusion coefficient of Nafion/SiO₂ composite membrane. *Chinese Journal of Power Sources*, (in press, in Chinese)
- Rodgers, M. P., Shi, Z. Q., et al. (2008). Transport properties of composite membranes containing silicon dioxide and Nafion (R). *Journal of Membrane Science*, Vol.325,No.1,pp. 346-356
- Santiago, E. J., Isidoro, R. A., et al. (2009). Nafion-TiO₂ hybrid electrolytes for stable operation of PEM fuel cells at high temperature. *Electrochimica Acta*, Vol.54,No.16,pp. 4111-4117
- Shao, Z. G., Joghee, P., et al. (2004). Preparation and characterization of hybrid Nafion-silica membrane doped with phosphotungstic acid for high temperature operation of proton exchange membrane fuel cells. *Journal of Membrane Science*, Vol.229,No.1-2,pp. 43-51
- Shao, Z. G., Xu, H. F., et al. (2006). Hybrid Nafion-inorganic oxides membrane doped with heteropolyacids for high temperature operation of proton exchange membrane fuel cell. *Solid State Ionics*, Vol.177,No.7-8,pp. 779-785
- Sumner, J. J., Creager, S. E., et al. (1998). Proton conductivity in Nafion 117 and in a novel Bis[(perfluoroalkyl)sulfonyl]imide ionomer membrane. *Journal of the Electrochemical Society*, Vol.145,No.107-110
- Tang, H., Wan, Z., et al. (2007). Self-assembled Nafion-silica nanoparticles for elevated-high temperature polymer electrolyte membrane fuel cells. *Electrochemistry Communications*, Vol.9,No.8,pp. 2003-2008
- Wang, K. P., McDermid, S., et al. (2008). Preparation and performance of nano silica/Nafion composite membrane for proton exchange membrane fuel cells. *Journal of Power Sources*, Vol.184,No.1,pp. 99-103
- Wang, L., Yi, B. L., et al. (2008). Pt/SiO₂ as addition to multilayer SPSU/PTFE composite membrane for fuel cells. *Polymers for Advanced Technologies*, Vol.19,No.12,pp. 1809-1815
- Wang, L., Zhao, D., et al. (2008). Water-retention effect of composite membranes with different types of nanometer silicon dioxide. *Electrochemical and Solid State Letters*, Vol.11,No.11,pp. B201-B204
- Xu, W. L., Lu, T. H., et al. (2005). Low methanol permeable composite Nafion/silica/PWA membranes for low temperature direct methanol fuel cells. *Electrochimica Acta*, Vol.50,No.16-17,pp. 3280-3285
- Yan, X. M., Mei, P., et al. (2009). Proton exchange membrane with hydrophilic capillaries for elevated temperature PEM fuel cells. *Electrochemistry Communications*, Vol.11,No.1,pp. 71-74
- Yang, C., Costamagna, P., et al. (2001). Approaches and technical challenges to high temperature operation of proton exchange membrane fuel cells. *Journal of Power Sources*, Vol.103,No.1,pp. 1-9
- Yen, C. Y., Lee, C. H., et al. (2007). Sol-gel derived sulfonated-silica/Nafion (R) composite membrane for direct methanol fuel cell. *Journal of Power Sources*, Vol.173,No.1,pp. 36-44

- Yonghao Liu, Baolian Yi, et al. (2005). Study on silicon oxide Nafion composite membranes for proton exchange membrane fuel cell operation. *Chinese Journal of Power Sources*, Vol.29, No.2, pp. 92-94, 112
- Yu, J., Pan, M., et al. (2007). Nafion/silicon oxide composite membrane for high temperature proton exchange membrane fuel cell. *Journal of Wuhan University of Technology-Materials Science Edition*, Vol.22, No.3, pp. 478-481
- Yuan, J. J., Zhou, G. B., et al. (2008). Preparation and properties of Nafion (R)/hollow silica spheres composite membranes. *Journal of Membrane Science*, Vol.325, No.2, pp. 742-748
- Zawodzinski, T. A., Jr., C. D., et al. (1993). Water uptake by and transport through Nafion® 117 membranes. *Journal of the Electrochemical Society*, Vol.140, No.4, pp. 1041-1047



Energy Storage in the Emerging Era of Smart Grids

Edited by Prof. Rosario Carbone

ISBN 978-953-307-269-2

Hard cover, 478 pages

Publisher InTech

Published online 22, September, 2011

Published in print edition September, 2011

Reliable, high-efficient and cost-effective energy storage systems can undoubtedly play a crucial role for a large-scale integration on power systems of the emerging “distributed generation” (DG) and for enabling the starting and the consolidation of the new era of so called smart-grids. A non exhaustive list of benefits of the energy storage properly located on modern power systems with DG could be as follows: it can increase voltage control, frequency control and stability of power systems, it can reduce outages, it can allow the reduction of spinning reserves to meet peak power demands, it can reduce congestion on the transmission and distributions grids, it can release the stored energy when energy is most needed and expensive, it can improve power quality or service reliability for customers with high value processes or critical operations and so on. The main goal of the book is to give a date overview on: (I) basic and well proven energy storage systems, (II) recent advances on technologies for improving the effectiveness of energy storage devices, (III) practical applications of energy storage, in the emerging era of smart grids.

How to reference

In order to correctly reference this scholarly work, feel free to copy and paste the following:

XiaoJin Li, ChangChun Ke, ShuGuo Qu, Jin Li, ZhiGang Shao and BaoLian Yi (2011). High Temperature PEM Fuel Cells Based on Nafion®/SiO₂ Composite Membrane, Energy Storage in the Emerging Era of Smart Grids, Prof. Rosario Carbone (Ed.), ISBN: 978-953-307-269-2, InTech, Available from:

<http://www.intechopen.com/books/energy-storage-in-the-emerging-era-of-smart-grids/high-temperature-pem-fuel-cells-based-on-nafion-sio2-composite-membrane>

INTECH

open science | open minds

InTech Europe

University Campus STeP Ri
Slavka Krautzeka 83/A
51000 Rijeka, Croatia
Phone: +385 (51) 770 447
Fax: +385 (51) 686 166
www.intechopen.com

InTech China

Unit 405, Office Block, Hotel Equatorial Shanghai
No.65, Yan An Road (West), Shanghai, 200040, China
中国上海市延安西路65号上海国际贵都大饭店办公楼405单元
Phone: +86-21-62489820
Fax: +86-21-62489821

© 2011 The Author(s). Licensee IntechOpen. This chapter is distributed under the terms of the [Creative Commons Attribution-NonCommercial-ShareAlike-3.0 License](#), which permits use, distribution and reproduction for non-commercial purposes, provided the original is properly cited and derivative works building on this content are distributed under the same license.